P297

For: *CLIMA 2000*, Brussels, Belgium, Aug. 29 - Sept 1, 1997.

Driving Rain on Building Facades

By: J.F. Straube[1] and E.F.P. Burnett[2]

Moisture is one of the most important factors affecting building envelope durability and performance, especially in cold climates. Understanding and predicting moisture movement within and through the envelope is therefore of fundamental importance. Although computer modelling of building envelope hygrothermal performance has made great strides in the last decade, one of the largest sources of moisture remains relatively poorly understood: driving rain.

The Building Engineering Group has conducted a number of studies of driving rain deposition, drainage, penetration, and absorption both in the lab and in a full-scale natural exposure and test facility. This paper presents some of the results from the detailed field monitoring of temperature and moisture, especially in brick veneers, of wall panels exposed to the climate of Ontario as well as laboratory tests.

The nature of driving rain is examined in some detail and theoretically-derived predictions are compared to field measurements. The coincidence of wind and rain especially with regard to seasonal and directional variations are considered. Driving rain deposition and wetting of vertical above-grade building envelopes is discussed and field results are compared to other research. The effects of rainfall intensity, rainfall duration, wind direction, previous wetting history, surface texture, and water absorption are discussed and some practical guidelines for the assessment of the driving rain moisture load are provided.

[1] Research Engineer, Building Engineering Group, University of Waterloo, Waterloo, Ontario, Canada, N2L 3G1.

[2] Professor of Civil Engineering and Director Building Engineering Group, University of Waterloo, Waterloo, Ontario, Canada, N2L 3G1.

1. INTRODUCTION

Moisture, regardless of source, is generally recognized as the most important agent of building enclosure deterioration. The amount of water deposited on the above-grade building envelope by driving rain is larger than any other source of moisture in almost all building types and climates. The deposited rain can result in staining, leakage, dimensional change, freeze-thaw damage, leaching, efflorescence, and biological deterioration. Water penetration of the cladding can cause similar problems in the interior parts of the wall. Despite the importance of driving rain to building performance, very little is known about the magnitude, duration, and frequency of driving rain and driving rain deposition on buildings.

This paper examines the mechanisms involved in driving rain and rain deposition on the vertical building envelope.

The volume of water deposited on a wall system is the result of the interaction between the wind, rain, the building, and the building envelope. The stochastic natures of the wind and rain, and the many variables associated with the building site and geometry makes the prediction of driving rain deposition on a wall a difficult task. Even if the rate of rain deposition on a building surface were known, the relative amounts of absorption, face drainage, and penetration of water will depend on the cladding material, texture, and previous wetting history.

The Building Engineering Group (BEG) is involved in a research program part of which involves the examination of the process of rain wetting, water penetration, and drying of cladding. Twenty-seven wall test panels, each 1.2 m wide and 2.4 m high, of ten different types have been built, instrumented, and installed in BEG's full-scale, natural exposure and test facility, the Beghut. Most of the test walls are light-gauge steel- or wood-framed assemblies clad with vinyl, EIFS, or clay brick veneer. The Beghut has standard meteorological instrumentation (wind, rain, temperature, relative humidity, solar radiation) as well as a total of 14 driving rain gauges on its walls and one mounted on a pole to the west of the building. Driving rain data has been continuously collected since November 1995.

The rain-wind-building interaction is examined in the following sections, based on previous research by others and supported by experimental measurements of Waterloo, Canada conditions. The wind, driving rain, and building interaction will be considered in three parts: the nature of driving rain, the coincidence of wind and rain for the test site, and how the building interacts with wind and rain.

2. DRIVING RAIN

Driving rain can be defined as the amount of rain that passes through an imaginary vertical plane. It is generally accepted that driving rain is primarily a function of windspeed and rainfall intensity, but rain drop diameter and the wind turbulence also play a role. The following sections will examine the nature of rain, the interaction of rain and wind, and the nature of the coincidence of windspeed, wind direction and rainfall.

2.1 Rain

Condensation of water vapour into cloud droplets (caused by cooling as a result of air rising) precedes rain. Cloud droplets are perfectly spherical in shape and range from 1 μm in diameter with an average about 25 μm [1,2]. Such small drops fall so slowly that their movement is completely governed by wind currents aloft and they act as suspended particles. When the drop diameter increases to more than about 0.25 mm, the drops begin falling.

If two rain drops in a rainfall touch, they will likely coalesce into larger drops. However, as the resultant drops become too large, aerodynamic forces overcome the surface tension forces holding the drop together and the drop will break apart (both Grey [1] and Beard [2] suggest that drops with diameters greater than about 6-7 mm are unstable). Therefore, as the rainfall intensity increases, the probability of two raindrops colliding increases and the average raindrop diameter increases. This conclusion is supported by the field measurements of Best [3], Laws and Parsons [4] and Marshall and Palmer [5] but each group developed its own relationship (Markowitz [6]). More recent researchers have made use of radar readings [7,8] and sophisticated electronic drop sizers [9,10] to further explore raindrops size distributions. The general conclusion of this body of research is that the nature of the distribution clearly varies not only with rainfall intensity but also with the type of storm, the cloud height, etc. Figure 1 is a plot of the relative probability distribution of raindrop diameter as a function of rainfall intensity given by Best [3]:

$$F(\emptyset) = 1 - \exp\left[-\left(\frac{\emptyset}{1.30 \cdot r_h^{0.232}}\right)^{2.245}\right] \qquad (1)$$

where, $F(\emptyset)$ is the cumulative probability distribution of drop diameters for a given rainfall intensity

$\emptyset$ is the equivalent spherical raindrop diameter (mm), and

r_h is the rainfall rate or intensity on a horizontal plane (mm/m^2/h).

While an accurate knowledge distribution of drop sizes may not be available, the physical characteristics of the drops themselves are well understood. Beard [2] recently collected the available experimental data of raindrop size, shape, and drag coefficient and, based on fluid dynamics principles, developed general relationships for the terminal velocity of raindrops as a function of air pressure and air temperature. These relationships match most available experimental data, including the comprehensive and widely accepted data of Gunn and Kinzer [11]. Figure 2 is a plot of this data. Dingle and Lee [12] developed a simplified equation, accurate to ±2.5%, for raindrop diameters of more than 0.3 mm: :

$$V_t(\emptyset) = -.166033 + 4.91844\emptyset - .888016\emptyset^2 + .054888\emptyset^3 \leq 9.20 \qquad (2)$$

where, $V_t(\emptyset)$ is the terminal velocity of a raindrop in still air [m/s].

More precise (± 0.5%) and much more unwieldy equations are available; see Beard [2].

2.2 The Interaction of Wind and Rain

All but the largest drops will reach their terminal velocity within about 20 m of beginning their fall [2, 11], i.e., for building applications it can be assumed that the drops are at terminal velocity. Similarly the horizontal velocity of the drops will equal the wind's within a short distance. The fraction of falling rain that will pass through a vertical plane is therefore:

$$r_v = r_h \cdot \frac{V}{V_t} \qquad (3)$$

where, r_v is the rate of rain passing through a vertical plane, i.e. driving rain (mm/m^2/h or l/m^2/h), and

V is the average wind velocity (m/s).

The mass of individual raindrops is sufficiently small that falling drops will respond to wind gusts of longer than about several seconds. Because the wind speed decreases significantly as the drop approaches the ground, the trajectory of a drop is curved. Very close to the ground (where the velocity changes quickly with height), at sharp changes in topography (e.g. hill tops),

and around buildings, the momentum of a drop will cause its velocity components to vary from that of the wind.

Lacy [13] conducted the seminal English-language field study of driving rain. He developed an equation by combining expressions of the median raindrop size as a function of rainfall intensity from Laws and Parsons [5] and the terminal velocity of such raindrops from Best [3]. The resulting relationship of wind speed and rainfall intensity to driving rain is:

$$r_v = 0.222 \cdot V \cdot r_h^{0.88} \tag{4}$$

Lacy's comparison of Equation 1 with 75 storms (of more than 10 hours duration and a total rainfall of more than 5 mm) showed a very good fit. Both because of the lack of other information, and the quality of the fit to the data, Lacy's equation has been the basis of almost all subsequent theoretical and field studies of driving rain.

Equation 1 is often simplified by assuming that driving rain is a simple linear function of wind speed and rainfall rate, i.e.,:

$$r_v = 0.222 \cdot V \cdot r_h = DRF \cdot V \cdot r_h \tag{5}$$

where, DRF is the driving rain factor (s/m).

The proportionality constant in Equation 5 relating rain on a vertical plane (driving rain) to rain on horizontal plane (falling rain) is defined here as the driving rain factor (DRF). From Equation 3 it can be seen that the DRF defined in equation 5 is:

$$DRF = \frac{1}{V_t} \tag{6}$$

Using an equation similar to Equation 5, Lacy [14] calculated a DRF of 0.208 at Garston, U.K. Based on many years of results Künzel [15] reported a DRF value of 0.20 for southern Germany, and Choi calculated a value of DRF = 0.228 for Sydney, Australia [16]. Equation 5 assumes a constant DRF and a linear relationship between windspeed, rainfall rate and driving rain. These assumptions form the basis of most of the world's driving rain maps.

2.3 Field Measurements of the Driving Rain Factor

A single free-standing driving gauge has been installed facing due west at a height 3.5 m above grade and 10 m upwind of BEG's test house. Of the more than 1000 15 minute periods during which it was raining, the DRF factor was calculated using equations 4 and 5 for the 147 periods during which the average wind direction was within 30° of due west. The values were adjusted for the cosine of the average wind angle off perpendicular during each period.

Many comprehensive measurements of raindrop size distributions (from ground and radar measurements) have found a considerable amount of scatter. Despite the scatter between individual results, the average DRF over all events was found to be 0.215, very similar to the other reported DRF values. As expected the DRF factor varied with rainfall intensity, because as the intensity increases, the drop size increases and so the terminal velocity increases. Table 1 compares the calculated DRF results (Equation 5) with the values calculated by Lacy's original relationship (Equation 4). The average in Table 1 is the weighted average for the number of samples in each of the four different rainfall intensity categories.

Rainfall Intensity (mm/h)	Number of samples (Wind ± 30°)	Measured DRF (Eqn 5)	Calculated DRF (Eqn 4)
< 1	43	0.272	0.244
1 - 2.99	55	0.220	0.237
3 - 4.99	23	0.188	0.223
> 5	26	0.136	0.187
Weighted Average	Sum = 147	0.215	0.228

Table 1: Measured DRF versus Lacy's Equation (4)

The results in Table 1 clearly show that ignoring the effect of raindrop size (as equation 5 does) will result in significant over predictions at high rainfall intensities, the degree of which depends on the proportion of high intensity rainfalls. As Choi [16] found, the DRF must be a function of rainfall intensity (or, more precisely, raindrop diameter).

Lacy used the following relationship of terminal velocity to rainfall intensity:

$$V_t(\emptyset) = 4.505 \cdot r_h^{0.123} \qquad (7)$$

The median raindrop diameter of each data set of each of the rainfall intensity categories in Table 1 was calculated using equation 1. The DRF was then calculated for each data point from the raindrop terminal velocity using both Dingle and Lee's relationship (Equation 2) and that used by Lacy (Equation 7). Table 2 presents the results. The agreement between the DRF calculated using Equation 2 is seen to be good, especially considering the expected accuracy of the experimental results and the imperfect equations of raindrop diameter distribution. Using a constant DRF value of 0.20 or 0.22 will obviously result in significant errors for all rainfall intensities other than 1-3 mm/h (the most commonly occurring rainfall intensity). If the median values are used to calculate the DRF, both equations are less accurate.

Intensity Category (mm/h)	Median Intensity (mm/hr)	Median Drop Diameter (mm)	Measured DRF (Eqn 5)	DRF Calculated using eqn 2	DRF Calculated using eqn 7
< 1	0.37	0.88	0.272	0.286	0.224
1 - 2.99	1.80	1.27	0.220	0.211	0.216
3 - 4.99	3.60	1.49	0.188	0.186	0.211
> 5	10.26	1.90	0.136	0.158	0.204

Table 2: Comparison of Measured DRF and Calculated DRF

Lacy's use of Equation 7 (based on the slightly inaccurate data of Laws and Parson) rather Equation 2 (based on the much more comprehensive and widely accepted data of Gunn and Kinzer) resulted in small errors in terminal velocity. Very small errors in predicting the terminal velocity will directly relate to the error in the DRF. Using the improved relationships for raindrop terminal velocity (Equation 2) and raindrop size distribution (Equation 1) obviously greatly improves the match between the experimental data compared to Lacy's equation. Lacy's equation likely fit his storm data well because the terminal velocity relationship of Equation 7 was reasonably accurate over the majority of rainstorm intensities he measured.

Although the DRF calculated using Equations 2 and 6 is typically within 5% of the measured data, it is in error by 15% for the highest rainfall category. The type of rainstorm affects the raindrop diameter distribution, and the majority of the high-intensity rainstorm data collected were during convective rainstorms (thunderstorms). The windspeed is also changing quickly with height at the gauge height of 3.5 m. Calculations show that the highest rainfall category contains a high percentage (> 50%) of rain drops large enough that they will fail to match the change in horizontal windspeed at the heights and windspeeds measured. If this is the case, it would mean that the equality in Equation 3 is no longer true. Until more data is analyzed it is unlikely that any further analysis can significantly improve this fit.

The change of the DRF with rainfall intensity is important for the extrapolation of driving rain data collected by researchers to the values needed for assessing likely extreme values. During rare rain events, say with intensities of more than 25 mm/h, the median drop size will be larger (2.3 mm), the terminal velocity higher (7 m/s) and the driving rain factor will therefore become quite small (0.140).

For routine, simple estimations of rainfall over longer averaging times, e.g. for the analysis of typical in-service conditions, equation 1 or equation 2 with a DRF of 0.22 are appropriate. For more detailed studies and for the assessment of extreme rain conditions, a more detailed approach may be warranted. Hygrothermal computer models which make use of detailed time-series weather files can, with little computational effort, calculate the driving rain approaching a building for every 15 min. or 1 hour period. Since real data appears to have a random scatter superimposed on the raindrop distribution, more sophisticated approaches could apply an appropriate random function to the raindrop distribution while remaining within the bounds of measured distributions.

3. THE COINCIDENCE OF RAIN AND WIND

Since driving rain is not routinely measured by weather stations, it would be useful to be able to predict the driving rain using the available and extensive records of rainfall and wind speed. It cannot, however, be assumed that the wind and falling rain can be modelled as statistically independent events. In fact, there is strong evidence to suggest that the wind-speed probability distribution is different during rain events [17], and it is well documented that the wind direction distribution is different during rain events [16, 17].

The wind, rain, and driving rain data collected at the test hut over a three season period (0301 to 1031, 245 days) was examined. Any day with more than 1 mm of total rainfall was considered a rainy day. A total of 77 days (31%) of the days were classified as rainy. Data from 15 minute periods was also analyzed. Of the 23238 15 minute averaging periods during the 245 days, rain was collected during 1088 (4.7%).

3.1 Windspeed During Rain

The relative probability distribution of the windspeed during rain and the windspeed during all periods is plotted in Figure 3. As expected, the windspeed follows a log-normal distribution. The windspeed during rain is only slightly higher in the mid-range but otherwise follows the same log-normal type of distribution. While these results cannot be used to support any sweeping generalizations, the more comprehensive study of standard weather records by Surry et. al. [17] also found a increase in windspeed, especially for small rainfall rates. Nevertheless, the increase is small (of the order of 10%) and the results support the use of the normal wind speed distribution as an approximation for the windspeed-during-rain distribution.

Choi [16], in his study of the area around Sydney, found that the use of annual values of the driving rain index (i.e. based on annual average wind speed x average annual rainfall) could result in significant (30-40%) under estimations versus indices based on hourly values.

Bear in mind that the distribution of *extreme* windspeeds during rain will be quite different than the normal windspeed distribution. In fact, the probability of the coincidence of very high windspeeds and high rainfall intensities is quite low because both events are relatively unlikely. Surry et al [17] found that the extreme windspeed during rain (any rain) was about 10 to 20% lower than the 1-in-10 year design speed for many Canadian locations. Choi also studied the joint probability of extreme wind and rain in Sydney [18]. He found that the windspeed during a 10 and 30 mm/hr rainfall were 73% and 29% of the 1-in-10 year speed respectively.

The seasonal windspeed-during-rain distribution for the test site was also investigated. The differences between the average windspeed distribution and the seasonal (spring, summer, fall) distributions were the same with and without rain. In all cases there was a bias toward slightly higher average wind speeds during rain. Finally, the windspeed-during-rain distribution was investigated for different rainfall intensities. Although there was no strong correlation between wind speed and rainfall intensity, it was clear that as rainfall intensity increased, there was a bias toward lower wind speeds, approaching those of the average. This trend was also supported by the climate analysis of Surry et. al. [17] for many locations.

The results of the above analysis suggest that the windspeed probability distribution during rainfall is not significantly different during rainfall, perhaps slightly higher, than during all times. Seasonal changes in wind speed distribution are also reflected in the windspeed-during-rain distributions. As the rainfall intensity increases, the windspeed is likely to be slightly lower. These results will, of course, depend on the meteorological causes of rainfall. Waterloo's climate is believed to be representative of many non-coastal, non-mountainous regions.

3.2 Wind Direction During Rain

The wind-direction-during-rainfall distribution was also analyzed. As is the case in many locations, driving rain is likely to come from different directions than wind during dry periods. Figure 4 shows the wind rose of the probability of wind from each direction during all hours and during rain. There is clearly a significant difference between the two wind roses. North American driving rain maps, however, provide a driving rain index that does not account for the different probabilities of direction. Similarly, the seasonal distribution is quite different. In Waterloo, driving rain is three times more likely to be accompanied by easterly winds than westerly winds in the spring, and southerly rains are only likely in the summer. The distribution of wind direction as a function of rain intensity showed that higher rainfall intensities could be expected from the east, and that light rainfalls were biased from the northwest.

Therefore, it can be concluded that the wind direction distribution during rain must be considered, both on an annual and seasonal basis if any reasonably accurate quantification of driving rain is desired. It is presumably for these reasons that some Scandinavian countries have calculated directional driving rain indices for different seasons and/or during periods when freezing could occur.

As a simple aid for the assessment of the combined influence of the wind and the rain, the Driving Rain Index (DRI) was defined by Lacy as the product of annual average windspeed and total annual rainfall. A more refined DRI was calculated from the present data using the 15 minute average values. The DRI so calculated will be exactly the same as the annual values if the windspeed-during-rain probability distribution is the same as the normal windspeed distribution. This index is plotted versus direction in Figure 5. While the index is essentially a plot of the wind speed during rain, when normalized with regard to directional probability, the plot shows that twice the average driving rain can be expected from east, while less than one quarter the average can be expected from the north. It is interesting to note that the largest directional value is about 10 times the smallest. Choi found the same range of values in his analysis of weather data in Australia [16].

3.3 Rainfall Duration and Intensity

The duration of rain fall also has a decided effect on the response of the building envelope. To assess the duration of rainfall, a rain event was defined as any period of rainfall during a day with a total of at least 1 mm rainfall and not interrupted by a period of longer than 12 hours. Using this definition, 60 rain events were so classified in the period considered.

The cumulative frequency of the rain event duration is plotted in Figure 6. As can be seen, the majority of events are less than about 8 hours long. Künzel [19], based on a different definition, found 60% of rain events at his South German location to be less than 8 hours long. These conclusions are sensitive to the choice of rain event definition, but do provide an indication of the range of durations that can be expected.

The average intensity of rainfall was found to be about 3.4 mm/hr, but the distribution was skewed to lower rainfall intensities so that the median value was 1.8 mm/hr. For hydrological calculations, intensity-duration-frequency curves are often used. Such a plot (Figure 7), based on long term meteorological data, shows that intense rain falls may occur for short periods of time, but, as expected, the intensity will decrease as the duration increases. Such plots are generally available and can be used to guide the choice of extreme rainfall intensities. As discussed earlier, windspeeds during extreme rainfalls are likely to be significantly lower than design values.

All of the above merely provides an outline of the influence site-specific weather and climate can have on driving rain calculations. Similar analysis can be conducted for any site given data with sufficient temporal resolution (preferably hourly). The exact nature of the rainfall-during-wind and wind-during-rainfall probability distributions need to be defined more accurately if driving rain at different sites are to be quantitatively assessed.

4. INTERACTION OF WIND, RAIN, AND THE BUILDING ENVELOPE

4.1 Background and Other Research

As the wind encounters a building, stream lines and pressure gradients form around the building. While it is clear that driving rain is re-directed by these streams of air, accounting for this effect is difficult.

A rain admittance function (RAF) is defined here as factor to transform driving rain at some horizontal distance (i.e. outside of the region disturbed by the building) to deposited rain on the building. The RAF accounts for the effect of the building on driving rain in the unobstructed wind and is believed to be a factor of the building's aerodynamics and the angle of attack of the wind. It is also likely that the RAF is a function of raindrop diameter and wind speed.

In his studies of driving rain on buildings, Lacy suggested that it might be possible to predict rain deposition on a building surface by applying a factor to the driving-rain intensity. The RAF is this factor. To predict driving rain deposition on the vertical face of a building an extension of Lacy's model of driving rain in the free wind can be written:

$$r_{bv} = RAF \cdot DRF(r_h) \cdot \cos(\theta) \cdot V(h) \cdot r_h = RAF \cdot \cos(\theta) \cdot r_v \qquad (8)$$

where r_{bv} is the rain deposition rate on a vertical building surface ($l/m^2/h$),

$V(h)$ is the wind speed at the height of interest,

θ is the angle between the normal to the wall and the wind direction, and RAF is the rain admittance function, where $RAF = r_{bv} \div (r_v \cdot \cos(\theta$

The literature contains only a few references of simultaneous measurements of driving rain in the environment and driving-rain deposition on a building. Recently, some researchers have pursued a computational fluid dynamics (CFD) approach [20] while others have begun wind tunnel modelling [21] to the help predict driving rain deposition on buildings.

The RAF has not been reported in most of the literature. However, it can often be calculated from published data. In most cases, the value of RAF is less than 1.0, and for low-rise, rectangular buildings the value near the center can be assumed to be about 0.3. Sandin [22, 23] reported values of 0.3 (near the lower centre) to 1.0 (upper corners) in studies of driving rain on low-rise rectangular buildings. Lacy [6] reported values of 0.3 for the middle, and about 0.5 for the corner of a low-rise wall over a wide range of wind speeds and rainfall intensities. Henriques [24] measured an RAF value of 0.6 on the centreline of a low-rise building, but the gauge was mounted near the top of the partially-obstructed building at an unreported height above the free-wind gauge. Flori [25] found a RAF value of almost 0.6 and, more importantly, reported increasing values of the RAF factor (up to 1.2) as the wind angle changed from normal to the wall to parallel to the wall.

These values of RAF have been calculated from driving rain measured at the same height in the free wind for low-rise (less than 10m) buildings. Higher up a tall building, the driving rain intensity will be higher because wind speeds increase with height according to a power law. Lacy's [6] measurements near the top corner of a highly-exposed ten-storey apartment building suggest a RAF value of 1.0. However, the amount of rain received a meter from the edge of the building appeared to be greater. Schwarz [26] measured driving rain deposition on an 18-story building for a seven-month period. The RAF factor was calculated to be 0.5 for the 10 m height. Windspeed increases with height following a power law distribution. Extrapolating windspeed data higher up the tall building studied by Schwarz (using the appropriate power law), one can calculate the RAF for other heights on the building from his data. The calculated RAF for the ninth and sixteenth storeys was no different than that for the third story at 10 m above grade. The RAF calculated for the upper corners of the building, however, ranged from 0.9 to 1.0. These results (RAF = 0.3 to 0.5 for the centre of a building and RAF = 0.9 to 1.0 for the corners) match Sandin's results for a low-rise building. An important implication of these results is that driving rain deposition increases with height at the same rate as wind speed. The RAF also appears to be scale-independent, probably in a similar way as mean wind pressure gradients can be scaled for buildings of the same geometry.

Note that all of the measurements reported above are averaged over several rain events, or even over several years. The RAF is likely to vary with the wind speed and rain drop diameters of the individual storm.

Choi's CFD model [20] was used to assess extreme events, and so the results are difficult to compare to the field measurements reported earlier. He calculated the amount of rain falling on a tall, narrow building with 3 zones horizontally and 4 vertically (a total of 12). For a 10 m/s windspeed and 10 mm/hr rainfall, he calculated a DRF of 0.48 in the top corner zone. Given the area over which the rain was calculated was equal to one-third the width and one-quarter the height, the RAF for smaller zones near the edges would likely be at least one. The importance of these theoretical RAF values is the trends exhibited by the RAF as a function of wind speed and rainfall intensity. Choi found that the RAF increased weakly with rainfall intensity (the maximum RAF increased by 25% for a fivefold increase in rainfall intensity to 50 mm/hr), and strongly with windspeed (a 70% increase over a 300% increase in windspeed). The RAF changed by a factor of less than 2 for a combined 300% increase in windspeed and 500% increase in rainfall intensity.

Although there is not a large amount of data available, Figure 8 is a summary plot of the largely consistent results available for RAF.

4.2 RAF Measurements

A total of 14 driving rain gauges are mounted on the four faces of BEG's test house. The east and west elevations of the building have six gauges each, while the north and south have one each. The total driving rain captured by the rain gauges mounted on the east and west elevation for the same period of 245 days analyzed earlier was used to calculate the RAF.

Using the actual measured amount of driving rain collected, the RAF was calculated for the total period for gauges on the west face. Similarly, using the DRF calculated as described earlier, the RAF for the gauges on the east face were calculated. Figure 9 plots these results.

A comparison of the RAF values in Figures 8 and 9 reveals some obvious and significant differences. The four upper corner gauges consistently have a much smaller RAF than expected. This is due to 2 factors. The plots in Figure 8 are based on results from buildings with blunt top edges. Hence, the flow over and around these buildings is characterized by high lateral and vertical accelerations of the air mass. The raindrops in the airflow will be unable to undergo this high an acceleration and so leave the airflow on a trajectory less steep than the wind. This results in a concentration of rain drops at corners and sharp changes. The peaked roof of the test building reduces the rate of acceleration required for the air mass to rise up and over the building. Since the sides of the hut are blunt, the mid-height corner gauges capture the expected amount of rain.

The test hut also has a small overhang (approximately 200 mm). Observation and the long-term experience of vernacular buildings suggests that an overhang helps control more than just near-vertical rainfall. By trapping upward flowing air near the top of the wall, an overhang will move the point of maximum vertical acceleration in the airflow further from the wall. Hence, when rain leaves the air flow, it is further from the wall and may fall downward, completely missing the wall. At high windspeeds this effect will be small, but for the majority of rain events, a significant reduction of average RAF may be achieved.

The beneficial effects of both overhangs and peaked roofs has qualitatively been observed in wind tunnel modelling of such buildings [21] and can have a significant beneficial effect on even relatively large buildings.

4.3 Rainwater on Walls

How water behaves once it strikes a wall is very dependent on the nature of the wall and, to some extent, the location of the wall on the building. Rain water deposited on the surface of a wall will either be shed (i.e., flow away along the outer surface of the wall), absorbed by capillarity into the wall material, or can penetrate further into the wall. To account for each possibility, a shedding/absorption/penetration (SAP) fraction is defined; it is merely the fraction of deposited rainwater that is dealt with by each of the three mechanisms.

If a porous building material becomes saturated, it will begin to behave like an impervious material; that is, any deposited moisture will simply be drained away. Therefore, the rate of water deposition, the material's moisture content, the surface absorption coefficient (itself a function of moisture content), the duration of the rain event, and the previous wetting and drying history of the cladding will all effect the SAP. The nature of surfaces above and beside the area of envelope being considered also play a role since water shed from these surfaces will add to the water on the wall.

If water is deposited on a vertical surface at a high rate, a surface film will form and ensure that any extra water will be drained away on the surface (i.e., shed). Claddings that have very low absorptions (e.g., metal, glass, polished granite) will drain a high ratio of deposited rain and increase the water load on the joints in the system. Joints in systems with little absorption will be exposed to an order of magnitude more water than the joints in walls with more absorptive

claddings (e.g., brick, wood). This behaviour is important because joints are still typically designed as perfect barriers, and field experience has shown that they rarely perform in this way.

The information on the typical duration and intensity of driving rain events presented in section 3.2 is useful to assess the likely behaviour of walls. Typical brickwork veneers can absorb a total of 5-10 kg/m^2 at rates of 1-5 kg/hr during a rain event before shedding. This suggests that many veneers will shed water only during statistically unlikely high intensity and/or long duration driving rain events. Water that is absorbed cannot penetrate and so the behaviour of brick veneers also provides a degree of rain penetration control. Glass and metal curtain walls, by contrast, will absorb no water and will have flowing water on their surface for almost all driving rain events. Hence, water penetration through the joints will always be more likely, simply because the joints are much more likely to be exposed to water.

5. CONCLUSIONS

The prediction of rain wetting of building facades, both under service and extreme conditions requires much more work. Methods to quantify the coincidence of wind and rain and the seasonal and directional changes in driving rain from existing long-term weather records should be developed. More detailed field measurements, both to confirm the present DRF calculations and to extend the existing body of RAF values are sorely needed, if only to calibrate and validate computer models and wind tunnel techniques. A significant amount of work remains to be done on the effect of windspeed, wind direction and rain intensity on the RAF.

Despite the caveats listed above, building designers and researchers are in a position to approximate, to within a factor of perhaps 2 or 3, the amount of driving rain likely to be deposited on a building either during a storm, over a season, or over a year. This knowledge can and should be used to properly design rain control measures and develop and implement appropriate test methods and performance models.

---

[1] *Handbook on the Principles of Hydrology*, ed. Donald M. Grey, National Research Council of Canada, 1970, pp. 2.2-2.3.

[2] Beard, K.V., "Terminal Velocity and Shape of Cloud and Precipitation Drops Aloft", *J. of the Atmospheric Sciences*, Vol. 33, 1976, pp. 851-864.

[3] Best, A.C., "The Size Distribution of Raindrops", *Quart. J. Royal Meteor. Soc.*, Vol. 76, 1950, pp. 16-36.

[4] Laws, J.O., and Parsons, D.A., "Relation of raindrop size to intensity", *American Geophys. Union Trans.*, No. 24, pt. 2, pp. 453-460, 1943.

[5] Marshall, J. S., and Palmer, W. M., "The distribution of raindrops with size", *J of Meteor.*, Vol. 5, Aug. 1948, pp.165-166.

[6] Markowitz, A.M., "Raindrop Size Distribution Expressions", *Journal of Applied Meteorology*, Vol. 15, pp. 1029-1031, 1976.

[7] Rogers, R.R., and Pilie, R.J.,"Radar Measurements of Drop-Size Distribution", *J. of the Atmospheric Sciences*, Vol 10, Nov. 1962, pp. 503-506.

[8] Caton, P.G., "A study of the raindrop-size distributions in the free atmosphere", *Quart. J. Royal Meteor. Soc.*, Vol 92, 1966, pp. 15-30.

[9] Dingle, A.N. and Hardy, K.R., "The description of rain by means of sequential rainddrop-size distributions", *Quart. J. Royal Meteor. Soc.*, Vol. 88, 1962, pp. 301-314.

[10] Bradley, S.G., and Stow, C.D., "The Measurement of Charge and Size of Raindrops: Part II. Results and Analysis at Ground Level", *J. of Appl. Meteor.* Vol 13, Feb 1974, pp. 131 - 147.

[11] Gunn, R, and Kinzer, G.D., "The terminal velocity of fall for water drops in stagnant air", *J. Meteor.*, Vol 6, pp. 243-248, 1949.

[12] Dingle, A.N., and Lee, Y., "Terminal Fall Speeds of Raindrops", *J. of Appl. Meteor.*, Vol 11, August 1972, pp. 877 - 879.

[13] Lacy, R.E., "Driving-Rain Maps and the Onslaught of Rain on Buildings". *Proceedings of RILEM/CIB Symposium on Moisture Problems in Buildings*, Helsinki, 1965.

[14] Lacy, R.E., "Driving Rain at Garston, U.K.", *CIB Bulletin*, No. 4, pp. 6-9, 1964.

[15] Künzel, H.M., *Bestimmung der Schlagregenbelastung von Fassadenflächen*. Fraunhofer-Institut für Bauphysik, Mitteilung 263, No. 21, 1994.

[16] Choi, E.C.C., "Parameters Affecting the Intensity of Wind-Driven Rain on the Front Face of a Building", *Proceedings of the Invitational Seminar of Wind, Rain, and the Building Envelope*, University of Western Ontario, London, Canada, May 16-18, 1994.

[17] Surry, D., Skerlj, P. , Mikitiuk, M.J., "An Exploratory Study of the Climatic Relationships between Rain and Wind," Final Report BLWT-SS22-1994, Faculty of Engineering Science, University of Western Ontario, London, September, 1994.

[18] Choi, E.C.C., "Determination of wind-driven rain intensity on building faces", *J. of Wind Eng. and Industrial Aerodynamics*, Vol 51, 1994, pp. 55-69.

[19] Künzel, H.M., *Regendaten für Berechnung des Feuchtetransports*, Fraunhofer Institut für Bauphysik, Mitteilung 265, 1994.

[20] Choi, E.C.C., "Determination of the wind-driven-rain intensity on building faces", *Journal of Wind Engineering and Industrial Aerodynamics*, Vol 51, 1994, pp. 55-69.

[21] Inculet, D.R., Surry, D., "Simulation of Wind-Driven Rain and Wetting Patterns on Buildings," Report BLWT-SS30-1994, Faculty of Engineering Science, University of Western Ontario, London, November, 1994.

[22] Sandin, K., "The Moisture Conditions in Aerated Lightweight Concrete Walls", *Proc. of Symposium and Day of Building Physics*, Lund University, August 24-27, 1987, Swedish Council for Building Research, 1988, pp. 216-220.

[23] Sandin, K., *Skalmurskonstruktionens fukt- och temperaturbetingelser*. Rapport R43:1991 Byggforskningsrådet, Stockholm, Sweden, 1991.

[24] Henriques, F.M.A., "Quantification of wind-driven rain - an experimental approach", *Building Research and Information*, Vol. 20, No. 5, 1992, pp. 295-297.

[25] Flori, J-P., *Influence des Conditions Climatiques sur le Mouillage et le sechalge d'une Facade Vertical*, Cahiers du CTSB 2606, Sept. 1992.

[26] Schwarz, B., "Witterungsbeansphruchung von Hochhausfassaden," *HLH* Bd. 24, Nr. 12, 1973, pp. 376-384.

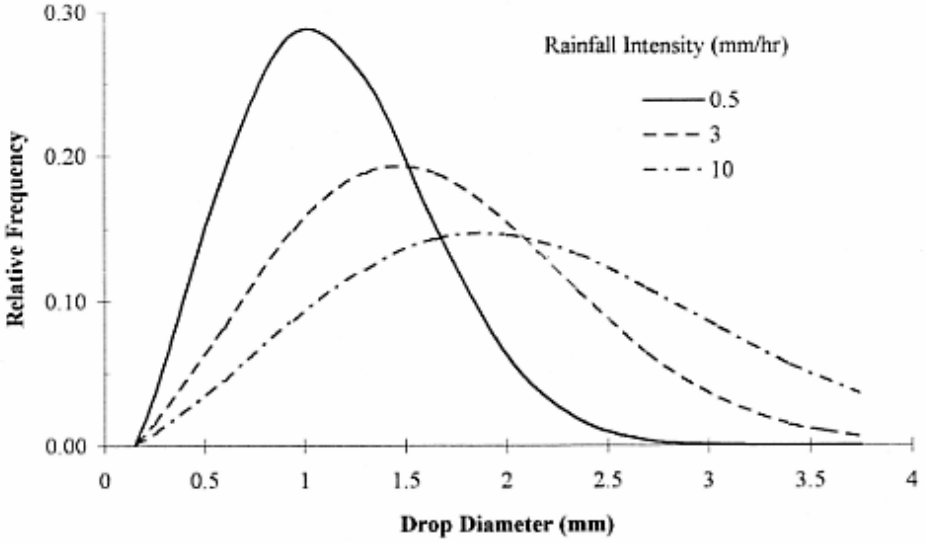

Figure 1: Distribution of Raindrop Sizes

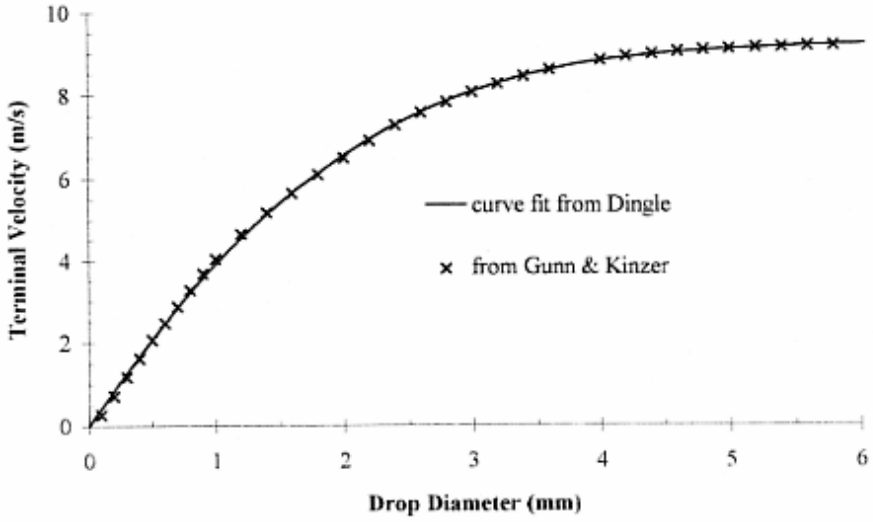

Figure 2: Terminal Velocity of Raindrops in Still Air

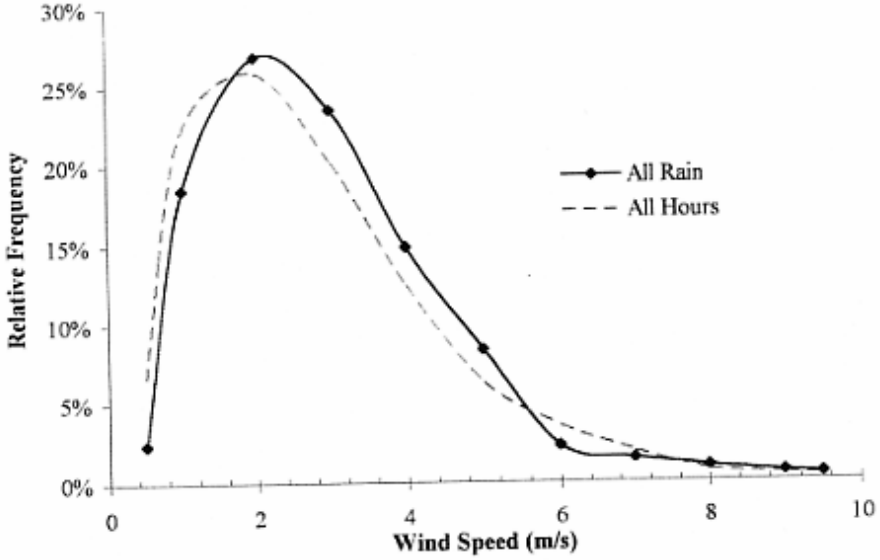

Figure 3: Windspeed Distribution During Rain and All Hours

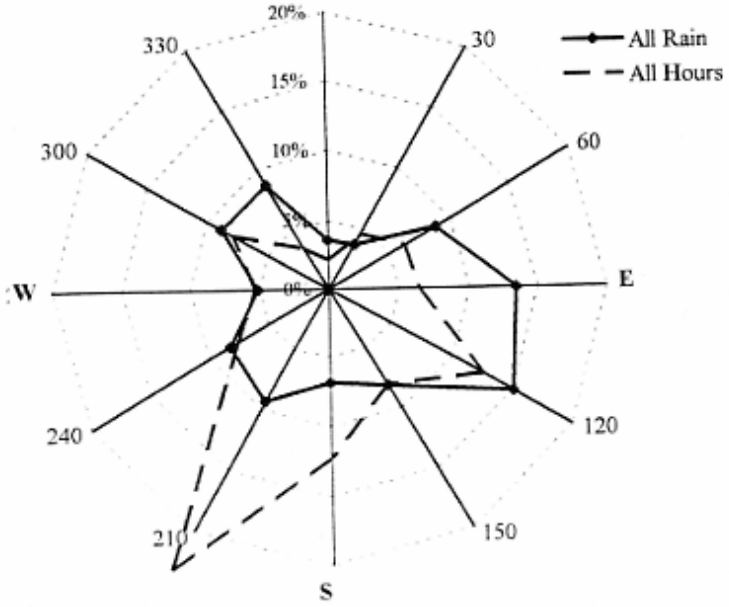

Figure 4: Wind Direction Distribution During Rain and All Hours

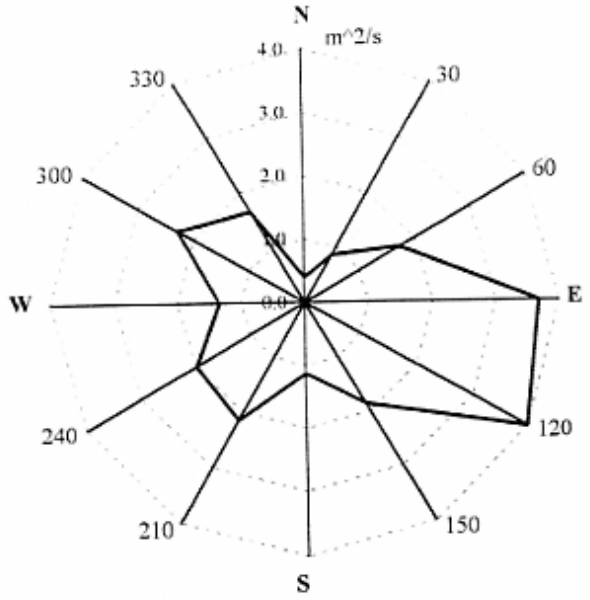

Figure 5: Driving Rain Index Corrected for Wind Direction Distribution

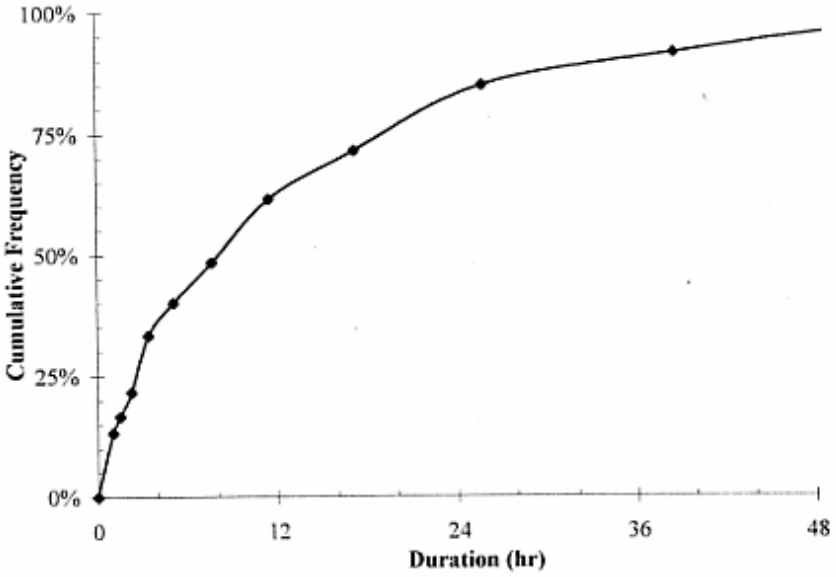

Figure 6: Cumulative Rain Event Duration Distribution

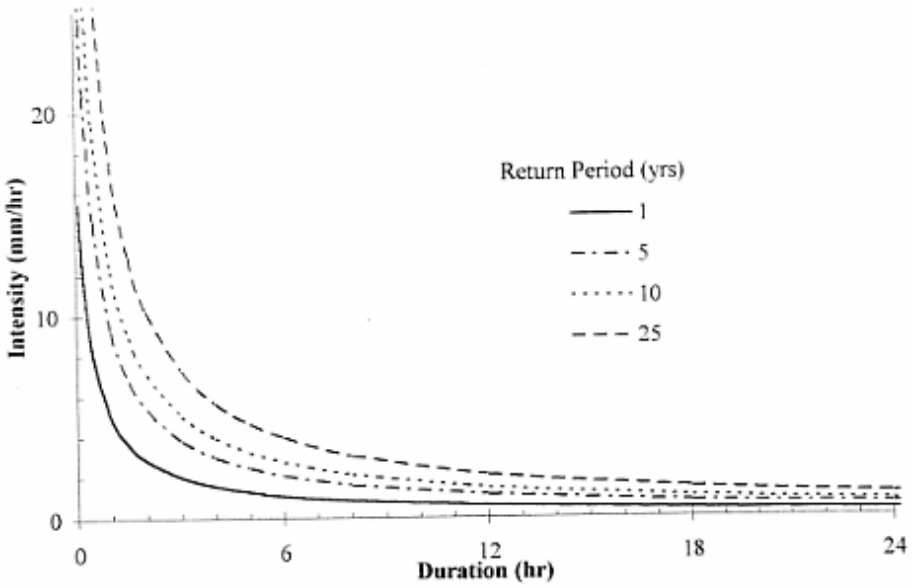

Figure 7: Intensity-Duration-Frequency Curves for Waterloo, Canada

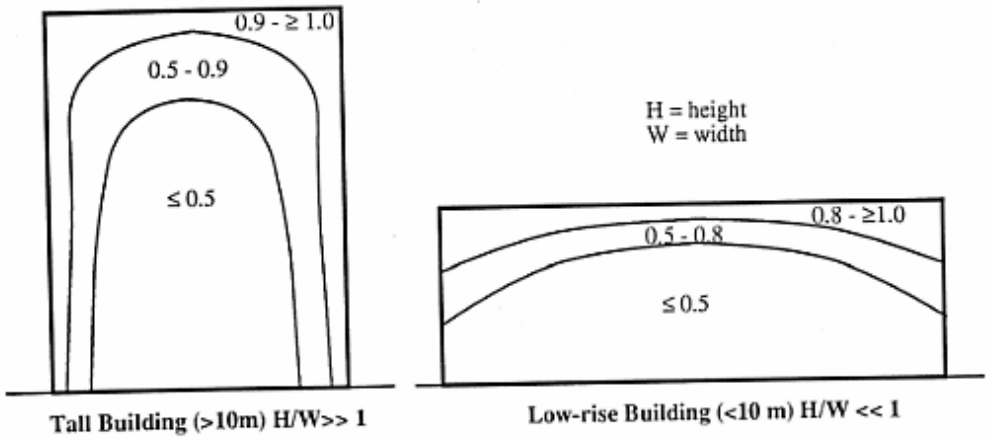

Figure 8: Summarized RAF Values From Other Researchers

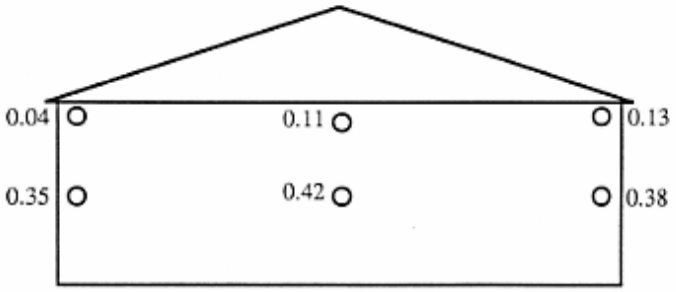

Measured Average RAF values for West Elevation

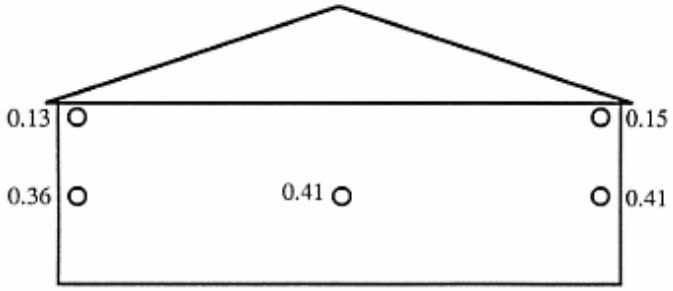

Measured Average RAF values for East Elevation

Figure 9: Measured RAF Values at Beghut